Surface Characterization and Its Role in Adhesion Science and Technology

9

John F. Watts

Contents

Abstract

This chapter reviews a variety of methods of surface characterization that have been found to be useful in the study of adhesion. The methods considered can be conveniently classified in three groups: those that provide information regarding surface topography (scanning electron microscopy and atomic force microscopy [AFM]); those that probe the surface-free energy of a material (measurement of contact angles and inverse gas chromatography, in addition to simple test methods such as the water break test and dyne inks); and those that provide a surface-specific chemical analysis (X-ray photoelectron spectroscopy, Auger

J. F. Watts (✉)
The Surface Analysis Laboratory, Faculty of Engineering and Physical Sciences, University of Surrey, Guildford, Surrey, UK
e-mail: j.watts@surrey.ac.uk

L. F. M. da Silva et al. (eds.), *Handbook of Adhesion Technology*,
https://doi.org/10.1007/978-3-319-55411-2_9

electron spectroscopy, and time-of-flight secondary ion mass spectrometry). All provide surface-specific information and this is essential for adhesion investigations as the forces responsible for adhesion operate over very short length scales and for any analysis to be meaningful the analysis technique must probe depths of a similar order of magnitude. These methods are used in all types of adhesion investigations, which, in general, can be considered in one of three areas of endeavor. The analysis of the unbonded surface and the relationship of surface characteristics to performance such as strength or durability, the forensic analysis of failed joints with a view to defining the exact locus of failure and any interfacial phenomena that may have exacerbated failure, fundamental studies of adhesion carried out with a view to gaining a fuller understanding of the interfacial chemistry of adhesion.

9.1 Introduction

The last three decades have seen many advances in our understanding of fundamental aspects of adhesion. This has led to a large body of data in the open literature that relates the surface characteristics of substrates and polymeric overlayers to the interfacial chemistry of adhesion, which, in turn, is used to establish structure/property relationships based on measurements of a performance parameter, at the fundamental level (such as the thermodynamic work of adhesion, see ▶ Chap. 6, "Thermodynamics of Adhesion"). For applied investigations, surface data will be related to more pragmatic quantities such as the performance of an organic coating in a salt spray test or the strength and more importantly the durability of a structural adhesive joint. One thing is clear, however, and that is the surface characteristics of the two phases have a profound influence on the formation of the interface, which in turn governs performance. Adhesion relies on the establishment of intermolecular forces between a substrate and the polymeric adhesive itself. To this end it is invariably necessary to pretreat the solid substrate in some manner to confer the required surface properties; this may be a simple abrasion treatment or a more sophisticated method such as acid anodizing. In a similar vein, chemical methods such as a corona discharge treatment and flame treatment used on polyolefins or the application of a primer solution based on an organosilane adhesion promoter may be used to ensure the required durability of an adhesive joint. In all cases the performance of the adhesive joint is directly related to the successful application of such a pretreatment, and an important part of the development of a new pretreatment procedure or the quality assurance of an established process is the assessment of the surface characteristics, both in terms of topography and chemistry.

The characterization that is necessary in order to begin to appreciate the complexities that exist at the polymer/metal oxide junction relates to both surface chemistry and topography. The aim of this chapter is to introduce methods that are now well established in the adhesion field; although it is not possible to provide a complete description of these techniques, the aim is to provide a general background of what can be achieved and indicate why such methods have become widely used in

adhesion investigations. At this juncture it is worth reflecting on what exactly one hopes to achieve by carrying out such investigations, a review of the literature establishes quite clearly that adhesion studies that involve surface characterization techniques essentially break down into three clear areas:

- The investigation of surface characteristics prior to bonding and correlation with some form of performance parameter
- The forensic investigation of failed adhesive joints and once again correlation of failure characteristics with a chosen performance parameter (see ▶ Chap. 43, "Techniques for Post-fracture Analysis")
- The use of sophisticated specimen preparation or modeling approaches to investigate the interfacial chemistry of adhesion

Such a list reflects the timeline along which adhesion science has developed in terms of surface characterization with the examination of the unbonded substrate being achieved first, then forensic analysis of failures and the determination of the interfacial chemistry of adhesion still being a significant challenge for many systems. Indeed the attainment of such a goal is in some ways the holy grail of adhesion science as it opens up the possibility of engineering the interface to provide a specific set of properties in terms of strength, toughness, and durability. Much headway has been made in this area in recent years but it is still a topic in which results are hard won and thus by definition very resource intensive.

The techniques by which such surface characteristics can be explored will be described in this chapter and a further chapter in this book will review the manner in which these methodologies are used in adhesion science (▶ Chap. 10, "Use of Surface Analysis Methods to Probe the Interfacial Chemistry of Adhesion"). The methods discussed will provide information regarding surface topography (SEM and AFM) as well as surface chemistry (XPS, ToF-SIMS, and AES). Surface thermodynamics is important at both a fundamental and an applied level and the use of wetting (see ▶ Chap. 4, "Wetting of Solids") and spreading (see ▶ Chap. 5, "Spreading of Liquids on Substrates") concepts such as contact angle and surface-free energy and inverse gas chromatography will also be considered.

9.2 Surface Topography

9.2.1 Scanning Electron Microscopy

Most laboratories engaged in adhesive bonding research and/or development will have ready access to scanning electron microscopy, and it is widely used to investigate both substrate surfaces prior to bonding and the characteristics of interfacial failure surfaces from adhesive bonds following a mechanical test. Optical or light microscopy is not really sufficient, not because it lacks the range of magnification of an SEM, although this is an important feature, but because of its poor depth of field and depth of focus. In optical microscopy features not in the image plane appear either under- or over-

focused (i.e., blurred) whereas an SEM is able to accommodate very large depths of field as exemplified by SEM images of small insects that often appear in the popular press. Having said that, the rigor of using digital photography to record all failure surfaces after test cannot be overemphasized to provide archival data that may provide important evidence once a program of testing has been concluded. As the general operating principles of an SEM are generally well appreciated, they will not be repeated here but the reader who needs a brief overview of operating principles is referred to standard texts such as Goodhew et al. (2001). The importance of surface topography is illustrated in Fig. 1. This shows a hot-dipped galvanized steel surface that has been temper-rolled (skin-passed) in readiness for a coil coating process. The surface rugosity is clearly observed at a scale of several tens of micrometers. As will be shown later in this chapter, the temptation to assume a homogeneous surface, although very natural, should be avoided as such mechanical treatment can lead to a well-defined heterogeneous surface.

It is very often convenient to use SEM to examine failure surfaces of joints as indicated above. The micrograph of Fig. 2 is the failure surface of an aluminum substrate bonded with a structural adhesive. Although on the basis of the microscopy one would tend to classify this as an interfacial failure, there are a few small islands of adhesive left on the metal side of the failure that vary in size from a few micrometers up to around 100 μm. As the polymer is an insulating material, it will generally charge during electron microscopy and this is evident in the micrograph of Fig. 2 as darker contrast around the adhesive residue. As ▶ Chap. 10, "Use of Surface Analysis Methods to Probe the Interfacial Chemistry of Adhesion" will indicate, the definition of the locus of failure is a rather complex task and depends on the level of sophistication of the assessment methods available, but for the time being the example of Fig. 2 will be considered an interfacial failure. Some pre-treatments lead to characteristic morphologies on a very fine length scale that can only be clearly defined by high-resolution SEM. The most widely cited example of this type of surface is the classic work of Venables (1984) on the morphology of acid anodized aluminum. The approach taken by these authors was to record stereo pair

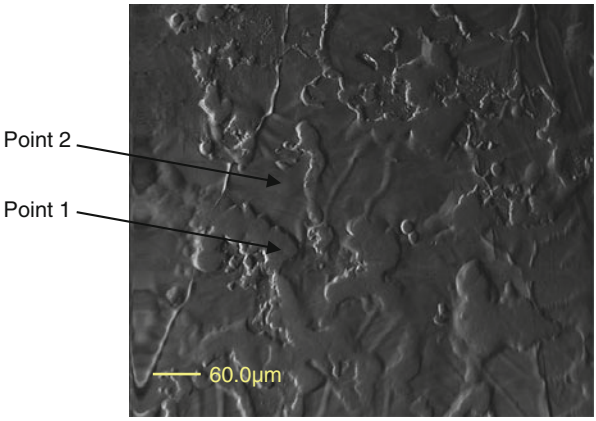

Fig. 1 Scanning electron micrograph of a hot-dipped galvanized steel surface

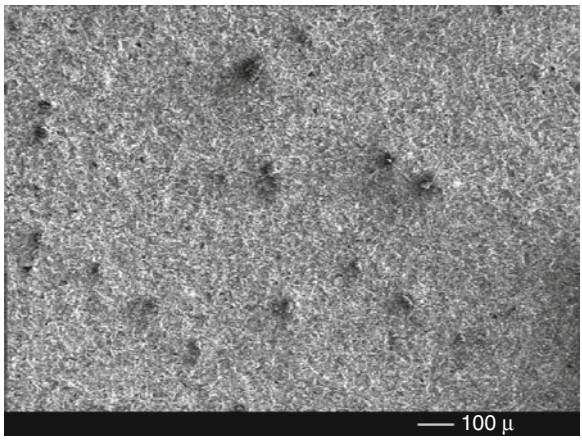

Fig. 2 The interfacial metal failure surface from an adhesively bonded aluminum test piece. The substrate has been grit blasted with 50 µm alumina grit prior to bond fabrication

SEM micrographs and present these along with an isometric drawing of the supposed morphology. These micrographs are, quite rightly, regarded as classics in the adhesion bonding literature and interested readers are referred to the above review of this work for further information.

In the case of polymeric substrates SEM is not quite so useful. The modifications brought about are quite subtle and the need to coat the insulating surface with carbon, gold, gold palladium, or a similar material to prevent electrostatic charging can add another level of complexity to sample preparation. Although useful for identifying debris at a surface or delamination in the case of composite materials, atomic force microscopy is generally preferred to SEM for the examination of polymer surfaces. SEM used in conjunction with energy dispersive X-ray analysis (EDX) will, however, always have a place in adhesion investigations as a result of the ready bulk analysis that can be undertaken, which will identify, for example, pigmentation in a coating or adhesive.

9.2.2 Atomic Force Microscopy

AFM is one of a family of techniques referred to by the generic name of scanning probe microscopy (SPM). These all have their genesis with the scanning tunneling microscope first developed by Binnig et al. (1982).

A schematic of an AFM is shown in Fig. 3, and although closely related to the STM the basic principle relies on the attraction between a sharp tip (often of silicon nitride) and the surface under examination. The tip is located at the free end of a cantilever of low spring constant (ca. 1 Nm^{-1}). The force between the tip and the sample cause the cantilever to deflect. A detector arrangement, based on a laser reflecting from the cantilever and a quadrant array photodetector, records the deflection of the cantilever as the tip is scanned relative to the sample. The extent of deflection of the cantilever can then be used to produce an image of surface

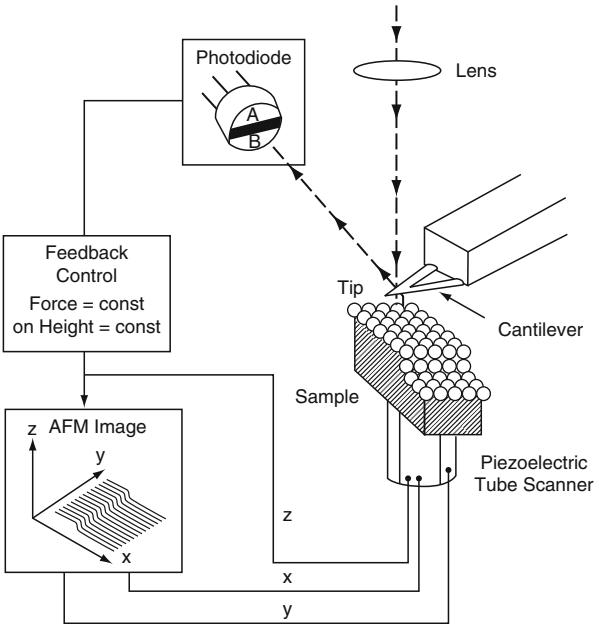

Fig. 3 Schematic of an atomic force microscope

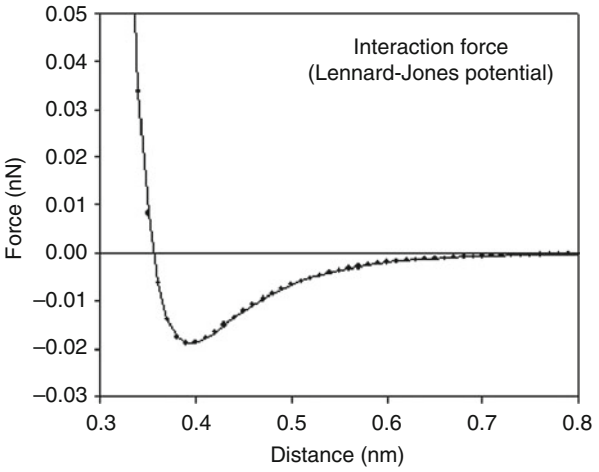

Fig. 4 Force curve showing interatomic force, between tip and specimen, as a function of distance

topography. The forces involved are repulsive at very close proximity (ca. 0.1 nm) but as the cantilever is withdrawn they become attractive as shown in Fig. 4. This leads to the definition of two forms of AFM operation, contact (ca. 0.2 nm distance on Fig. 4) and noncontact AFM (0.4–0.6 nm). In contact AFM, the tip makes gentle contact with the sample and, in the case of very soft or delicate samples (e.g., pressure sensitive adhesive tape) may indent the surface giving erroneous results, if any at all. To overcome this problem the tip may be vibrated near the surface

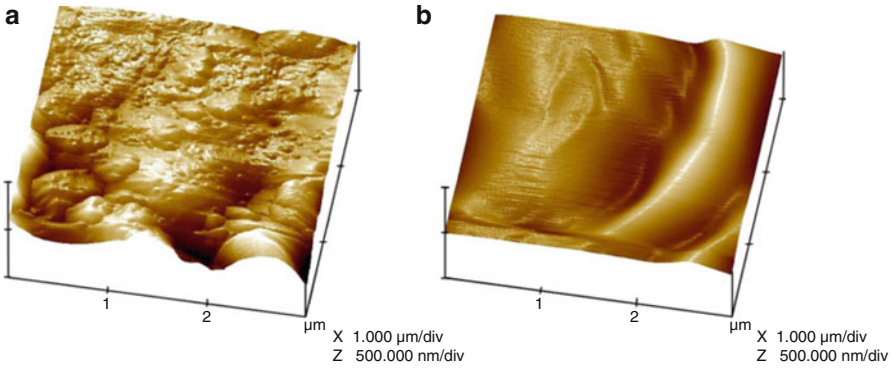

Fig. 5 Tapping mode AFM image of a commercial PVC extrudate: (**a**) before treatment and (**b**) after flame treatment

(1–10 nm); however, the force between tip and sample may be very small (10–12 N) making it more difficult to measure than the force in the contact mode, which is several orders of magnitude higher. There is also the possibility of the tip being pulled into the sample so stiffer cantilevers are required. A compromise between these two modes of operation is tapping mode AFM (TM-AFM) in which a sinusoidal vibration is applied to the tip and it gently taps against the surface; as shear and lateral forces are reduced, sample damage is, in most cases, negligible. An example of TM-AFM is shown in Fig. 5, which illustrates the topography of a poly (vinyl chloride) (PVC) surface before and after energetic surface treatment.

AFM has a wide range of magnifications from close to atomic resolution to a magnification of approximately 500 times; so in many ways it competes with the SEM as a method of assessment of surface topography. The complementarity of AFM and SEM have been discussed at some length by Castle and Zhdan (1997). Instruments are now available in portable format, low cost versions, geometries to accommodate very large specimens, and a plethora of different versions handle difficult samples such as cells and wet surfaces, making it a very versatile technique indeed. As far as those involved in adhesive bonding are concerned, the advantages of an AFM over other forms of surface characterization are threefold: Firstly, all samples, metal, polymer, ceramic, viscoelastic adhesives, and so on, can be handled successfully without the need for further sample processing. Secondly, by processing the image data as a line scan it is possible to carry out a "sectional analysis" that is essentially stylus profilometry, as described in BSI (2010) at the nanometric scale. The third is rather more specialized but if one measures forces directly one can use the AFM to monitor forces and thus use it as a localized surface forces apparatus, probing the adhesion properties of a polymer blend, for instance. In a similar manner force modulation can be used to probe localized elastic properties in the cross section of a polymer composite, or adhesive joint, and in this manner an interphase zone can be identified mechanically. Such modes of operation complement the traditional ways of probing surface-free energy, which are discussed in the following section.

9.2.3 White Light Interferometry

Although AFM has much to recommend itself as a technique for surface characterization, its primary role in most areas of research is, as its name suggests, that of a sophisticated microscope for the elucidation of surface topography. As a means of the determination of surface roughness it remains something of "an overkill," but in addition it has two significant disadvantages for roughness measurement. Firstly, AFM is still some way off becoming a routine tool for quality assurance with a high level of operator skill being required, in addition the speed with which data is produced is not high and given the choice of an SEM or AFM for initial assessment of a surface many operators would resort to the rapidity of the former. The upper bounds of measurement achievable may also be a problem with samples exhibiting coarse features, as for AFM the scan area in the x and y directions is limited to tens or at best hundreds of micrometers and in the z direction only a few micrometers. The solution to the need to acquire statistically meaningful measures of surface roughness over relatively large areas has been driven by the microelectronics industry, which has the need to assess large wafers at roughnesses of much less than 1 nm. The solution to this need has been the development of the well-established technique of white light interferometry (WLI) into a routine quality assurance procedure, with large ranges available in all axes and superb height resolution (0.01 nm are quoted for the latest instruments). The area where AFM outperforms WLI is in lateral resolution, although for many measurements of relevance to adhesive bonding this will not present a problem.

The background to optical interferometry is well known and is based around the spitting of a beam from a single light source into two separate beams using a beam splitter: one of the beams acts as a reference and follows a well-defined path and the other is reflected from the sample surface. At some point in the optical path, the two beams recombine to form an interference pattern of light and dark fringes. This is then magnified by the detector optics and finally imaged using a suitable device such as a CCD (charge-coupled device) camera. If at the same time the objective lens is moved vertically (to change path length between sample and beam splitter), with a high-resolution device such as a piezoelectric drive system, a series of dynamic interference fringes will be observed. Constructive interference will lead to a brightening of the image and, provided the movement of the objective lens is known accurately, this can be mapped back to a position on the sample surface via the establishment of the brightest point on each element of the CCD array. In this way it is possible to create a three-dimensional image of the sample surface by recording the position of the objective that gives the brightest image at each point on the CCD. Data from WLI is often presented in the form of a color-coded topographic plot or a pseudo three-dimensional plot, forms that are familiar to many as a result of their popularity with AFM manufacturers. Roughness values will be reported usually as an average over the entire field of view rather than the one-dimensional line familiar from stylus profilometry or sectional analysis in the AFM.

9.3 Surface Energetics

9.3.1 Simple Test Methods

Surface energetics is the behavior of gas and liquid molecules on solid surface and the relationship to the surface-free energy of the solid and liquid phases. The three-dimensional equilibrium packing of solids and liquids cannot be maintained at the surface and this less-than-satisfactory situation gives atoms at the surface a greater free energy than those in the bulk. This excess energy is known as the surface-free energy and has the units of energy per unit area, and using the SI notation surface-free energy, represented by the symbol γ, is always reported in mJm^{-2}. In liquids the surface-free energy gives rise to the well-known phenomenon of surface tension and, indeed, the values of surface-free energy and surface tension are numerically equal, although surface tension has the units of force per unit length, in the SI notation mNm^{-1}. It is incorrect to refer to the surface tension of a solid and terms such as wetting tension, interfacial tension, and so forth are now regarded as deprecated. The value of surface-free energy can vary widely: solid polymers represent the lowest class of solid materials with values in the range of 20–50 mJm^{-2}, inorganic solids have values in the range of 100 s mJm^{-2}, while clean metal surface (which are not achieved in practice except for the noble metals) are in the range of 1000 s mJm^{-2}. Liquid water, as a result of the hydrogen bonding present, has an unusually high-value surface-free energy for a liquid at 72 mJm^{-2} (or a surface tension of 72 mNm^{-1}!). Solid polymers on the other hand are characterized by very low values of surface-free energy as the surface of polymers generally do not contain broken bonds (or unsatisfied valencies) but merely loops resulting from the folding of the macromolecules making up the polymer structure. Thus the energy difference between bulk and surface is relatively small leading to a small value of surface-free energy.

As with bulk surface thermodynamics there is a driving force to reduce the surface-free energy of a material. For a solid such as a metal oxide this is readily achieved by the adsorption of a monolayer of organic vapor from the ambient. As surface practitioners are only too aware, any high-energy surface will adsorb such a monolayer spontaneously and all samples of this type analysed by X-ray photoelectron spectroscopy (or other methods for surface chemical analysis) will show tell-tale signs of the adsorption of adventitious carbon in the spectrum. The reduction of surface-free energy is the driving force for the deposition of a well-defined hierarchy of layers as discussed in detail by Castle (2008).

Any technique that probes explicitly, or at least gives an indication of the value of surface-free energy, has the potential to provide information regarding the behavior when a solid surface is coated with a liquid such as an adhesive or organic coating. Such measurements will be extremely surface sensitive, mostly providing information about the outer one or two atomic layers. Such methods can be used in a very pragmatic manner for quality assurance and also in a much more sophisticated manner using well-established protocols to evaluate surface-free energy and deduce the contribution to the parameter from various bonding types.

In the category of simple quality assurance methods, there are two widely used tests that provide straightforward information about the fitness of a solid surface (inevitably after treatment) for further processing: dyne pens and the water break test. Dyne pens are used for the assessment of polymeric surfaces where pretreatment has been carried out to increase the surface-free energy of the material by the incorporation of more polar functional groups. The concept of dyne markers is extremely simple (the term dyne is the cgs unit of force, surface tension having the units of dyne $cm^{-1} = mNm^{-1}$; 1 N = 10^5 dyne; this system of units is based on centimeter-gram-second units and was the predecessor of the SI or mks system based on meter-kilogram-second units). They are usually supplied as a kit containing pens with "inks" of well-defined surface tensions, usually between 30 and 60 mNm^{-1}. In order to assess the surface under test, and they are used almost exclusively to establish the printability of polymer surfaces following surface treatment, the marker pen is applied to the substrate, and if it marks (i.e., the liquid wets) the surface then the substrate has been treated to a level required for wetting to take place. These markers will always have a dye included in the liquid so they can be used in the conventional sense as marker pens for product identification. In general these markers will be used as a go/no-go during processing or to identify the treated side of a polymer film. By using a range of dyne pens, it is possible to estimate the surface tension of a liquid that will just wet the surface and thus gain an indication of the level of treatment of the polymer surface. The advantage of this system is that it is quick, cheap (<€10 per pen), easy to use, and, if the pen is new, can provide quite accurate results. The drawbacks are the short shelf life of pens, easy contamination of the liquid, and the lack of a numerical value relating directly to substrate properties – only a relative ranking order can be deduced. Notwithstanding such shortcomings, dyne markers will continue to play an important role in the surface treatment industry.

The other widely used simple test method is the water break test as described in ASTM (2002). The purpose of this test is to assess the efficacy of a cleaning process of a metal substrate. Here the requirement is exactly the opposite to that for the assessment of polymers in that an oxidized metal surface will have a high surface-free energy that may be compromised by the adsorption, or indeed a deliberate application of organic vapors or liquids. Cleaning is required to remove such extraneous material, which leads to a higher surface energy, and the successful removal of contamination is easily recognized by this test. Such carbonaceous films will be hydrophobic (non-wetting) in nature and the test involves withdrawing the metal panel under test from a container full to the brim with distilled water. On withdrawing a clean substrate, the water will drain uniformly over the surface. In the presence of residual contamination the draining water film will break up into a discontinuous layer around the contaminated regions. Although this is a very subjective test it is quick to carry out and lends itself to process control purposes. One form of the test is embodied in an international standard.

However, it is the measurement of contact angle that provides the most sensitive method and one that can be adapted to provide a quantitative measure of surface-free energy.

9.3.2 Contact Angle

The observation of contact angle (θ) can be related to the surface-free energies of solid substrate (γ_{solid}) and wetting liquid (γ_{liquid}), along with the interface free energy ($\gamma_{interface}$) by the well-known Young Equation:

$$\gamma_{solid} = \gamma_{liquid} \cos\theta + \gamma_{interface} \quad (1)$$

which by the simple expedient of resolution of forces about the triple point relates the surface and interface free energy terms to the observed contact angle as shown in Fig. 6. This observation of a sessile drop is frequently used as a quality assurance measure as a very low water contact angle indicates a hydrophilic surface (i.e., one with a relatively high surface-free energy) and a high contact angle indicates a hydrophobic surface (low surface-free energy). The observed contact angle is simply a measure of the propensity of the liquid (generally water in a simple test) to bond with itself compared with the solid substrate. For a hydrophobic substrate the hydrogen bonding between water molecules is much greater than the association between water and the substrate; in the case of a hydrophilic substrate, the association between water molecules and substrate is sufficient to overcome the hydrogen bonding responsible for the self association between water molecules. The direct observation of a large sessile drop (several millimeters in diameter) is readily accomplished in a production environment but the results obtained are only representative of the actual surface-free energy of the substrate if the substrate is homogeneous; heterogeneities in either topography or composition may prevent equilibrium being attained as required by the Young Equation. This may lead to the periphery of the drop departing from the circular and such behavior also manifests itself as contact angle hysteresis. This is often the case and the use of a sessile drop deposited by syringe or pipette has limited the use of contact angle measurement in such environments. Recently, however, the concept of ballistic sessile drop deposition, in which a stream of nanoliter volume drops are deposited on the surface and then coalesce into a single drop with a volume of several microliters, has been investigated and developed to the point that such a device is now available commercially under the name Surface Analyst™ from Brighton Technologies Group Inc. (2010). The output from the device is the diameter of the drop deposited in this manner, typically of the order of several millimeters. Initial results are extremely promising and show that such a device is able to separate

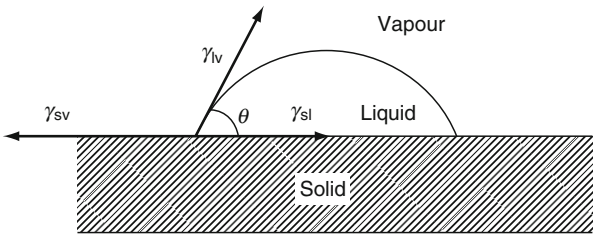

Fig. 6 The equilibrium that exists between a sessile drop and a solid surface, indicating the contact angle

composite panels prepared for adhesive bonding and then contaminated with a range of typical liquids found in a production plant (Dillingham et al. 2010).

As discussed above the surface-free energy of the probe liquid will influence the extent of solid–liquid interactions which will be observed as the contact angle. By the simple expedient of using a range of liquids with different surface-free energies and bonding types, it is possible to use such an approach to determine the surface-free energy of the solid. Many commercial instruments are available and all will be supplied with a dedicated computer that will contain the necessary software to make calculations of surface-free energy and related parameters, although all software should be supplied with a health warning for the inexperienced user! It is possible to assess the surface-free energy by extending the Young Equation, above, and recognizing that the surface-free energy can be subdivided into components that represent the degree bonding attributable to dispersion forces (γ^{D}), polar forces (γ^{P}), hydrogen bonding (γ^{H}), and so forth, such that:

$$\gamma = \gamma^{D} + \gamma^{P} + \gamma^{H} + \ldots \tag{2}$$

where the exact number of components depends on the material type and thus the bonding types involved. It is possible to arrive at the following relationship, the derivation of which is given by Packham (2005):

$$1 + \cos\theta = 2\frac{\left(\gamma_L^D \gamma_S^D\right)^{1/2}}{\left(\gamma_L\right)} + 2\frac{\left(\gamma_L^P \gamma_S^P\right)^{1/2}}{\left(\gamma_L\right)} \tag{3}$$

where the subscripts S and L represent the solid substrate and wetting liquid, respectively. The approach involves the use of a series of liquids of known values of the dispersive and polar contributions to surface-free energy, to measure the contact angles on the solid substrate of interest. This then yields a number of simultaneous equations of the type shown above. As they contain only two unknowns, the dispersive and polar contributions of the surface-free energy of the substrate, these can be readily evaluated. An alternative approach is to rearrange the equation in the form:

$$\frac{\gamma_L(1 + \cos\theta)}{2\left(\gamma_L^D\right)^{1/2}} = \left(\gamma_S^P\right)^{1/2}\left[\frac{\left(\gamma_L^P\right)^{1/2}}{\left(\gamma_L^D\right)^{1/2}}\right] + \left(\gamma_S^D\right)^{1/2} \tag{4}$$

The equation is now in the form of $y = mx + c$, and a graph of $\gamma_L(1 + \cos\theta)/2\left(\gamma_L^D\right)^{1/2}$ plotted versus $\left[\left(\gamma_L^P\right)^{1/2}/\left(\gamma_L^D\right)^{1/2}\right]$, the gradient of the best-fit line will be $\left(\gamma_S^P\right)^{1/2}$, and the line intercept $\left(\gamma_S^D\right)^{1/2}$. The surface energy of the unknown solid, γ_S, is then the sum of the two terms, $\gamma_S = \gamma_S{}^D + \gamma_S{}^P$. The form of plot obtained using this approach is illustrated in Fig. 7, which represents data obtained from a poly (dimethyl siloxane) surface using water, di-iodomethane, and hexadecane as probe liquids that gave mean contact angles of 119°, 79°, and 37°, respectively.

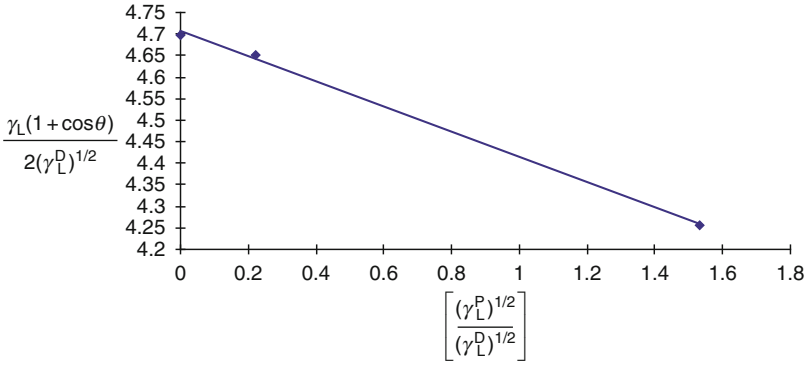

Fig. 7 Wetting data for poly(dimethyl siloxane) (PDMS) probed by water, di-iodomethane, and hexadecane

Table 1 Surface-free energies of liquids used in the wetting experiment of Fig. 7

Probe liquid	γ^D (mJm^{-2})	γ^P (mJm^{-2})	γ (mJm^{-2})
Water	22	51	73
Di-iodomethane	28	0	28
Hexadecane	2	49	51

The relative contributions of dispersion and polar bonding to these three liquids are shown in Table 1. The value of surface-free energy obtained in this way was 22 mJm^{-2} (Choi 2003).

9.3.3 Inverse Gas Chromatography

As shown above the use of contact angle measurements provides a relatively straightforward manner in which to assess the surface energetics and wetting characteristics of a solid surface. It is particularly attractive as it can be used on several levels of complexity ranging from a qualitative assessment of surface behavior (hydrophobic or hydrophilic) through to its use for the determination of surface-free energy and relative contributions to that parameter from dispersion and polar bonding. In spite of these obvious advantages it remains a macroscopic measurement and invariably represents the value over a large area, and application to rough surfaces will suffer from excessive amount of contact angle hysteresis unless some form of ballistic drop deposition is employed. An alternative approach to assessment of surface-free energy of solids is the use of inverse gas chromatography (IGC). The term inverse is used in the title to indicate that the material of interest is the stationary phase in the gas chromatography column rather than the volatile species injected into the column. (In the usual mode of operation for gas chromatography the volatile species is the phase under investigation and a standard stationary phase is employed.) The major restriction of IGC is that the solid phase under investigation

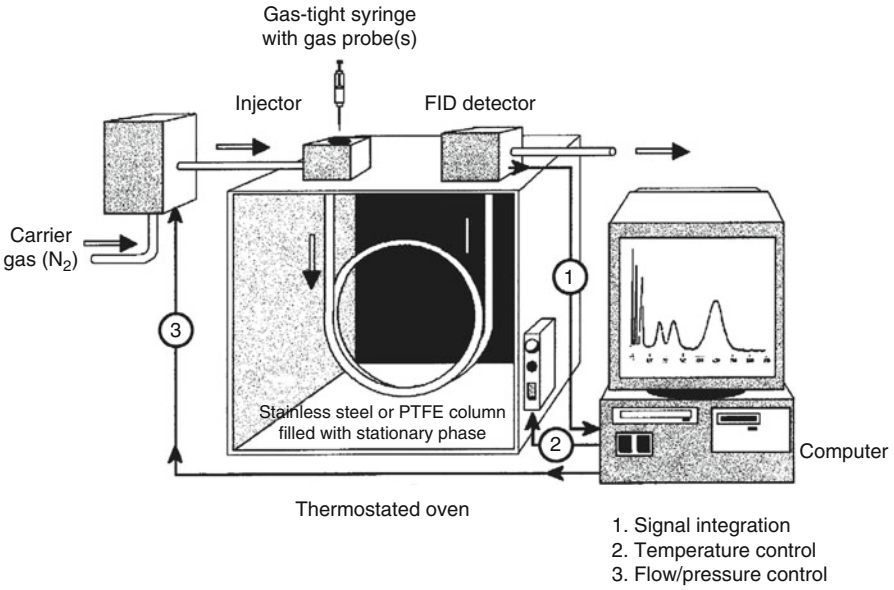

Fig. 8 Schematic diagram of the experimental configuration used for inverse gas chromatography (Reproduced from Abel and Watts 2005a with permission)

must be in a form suitable for incorporation into a column a few millimeters in diameter. This limits the physical form to coarse powders and fibers. As the stationary phase is usually conditioned at elevated temperature (ca. 120 °C) before injection of probes, this provides the driving force to desorb adventitious contamination and water so that adsorption of the probes is carried out on a cleaner surface than contact angle measurements. One advantage of IGC is that the high-energy sites on the surface are probed preferentially and rough surfaces can be investigated; indeed the comparison of results from long chain and branched isomers of the same molecule (usually an alkane) enable roughness to be elucidated.

The form of a typical IGC arrangement is shown in Fig. 8 and is readily carried out using standard GC equipment although specialized IGC equipment is available that allows the control of relative humidity and automated operation (Surface Measurement Systems 2010). A column of stainless steel or poly(tetra fluoroethyene) (PTFE) is packed with the solid of interest and loaded between the injector and the detector. The analytical measurements consist of injecting, sequentially, a series of volatile probes of known properties through the column along with an inert carrier gas. The retention time for each probe is related to the surface properties of the stationary phase. The usual practice is to carry out a series of injections with a homologous series of nonpolar organic probes such as the n-alkanes. This gives information about the interactions between the probes and the stationary phase associated with dispersion forces (sometimes referred to as Lifshitz–van der Waals forces). When a parameter derived from the observed retention time is plotted against probe boiling point, a logarithmic relationship can be observed which can be used to calculate the dispersion

bonding contribution to surface-free energy (Abel and Watts 2005a). Alkane probes are apolar molecules only able to interact with solid surfaces through dispersion bonding and for this reason they only probe dispersion interactions with the stationary phase enabling the contribution of this bond type to surface-free energy to be assessed. In order to assess the contribution of acid–base (or polar) interactions it is necessary to use polar probes, the magnitude of the deviation from the linear relationship referred to above being a measure of the magnitude of acid–base interaction between the stationary phase and the polar probes (Abel and Watts 2005b). The effect on retention time of the probe properties is illustrated in Fig. 9, which is an inverse gas chromatogram achieved by simultaneously injecting five probes (two alkanes and three polar probes) and methane as a noninteracting marker to define zero time. The substrate is hydrated alumina. A typical plot achieved in this manner is shown in Fig. 10 for an aromatic methacrylate resin (the parameter V_N in the ordinate is the net retention volume which is calculated from the net retention time, the primary measurement in IGC, illustrated in Fig. 9). The three polar probes are a combination of acidic and basic types: trichloromethane is acidic, ethyl acetate amphoteric but predominantly basic, and tetrahydrofuran is basic. The fact that significant deviations are seen from the reference

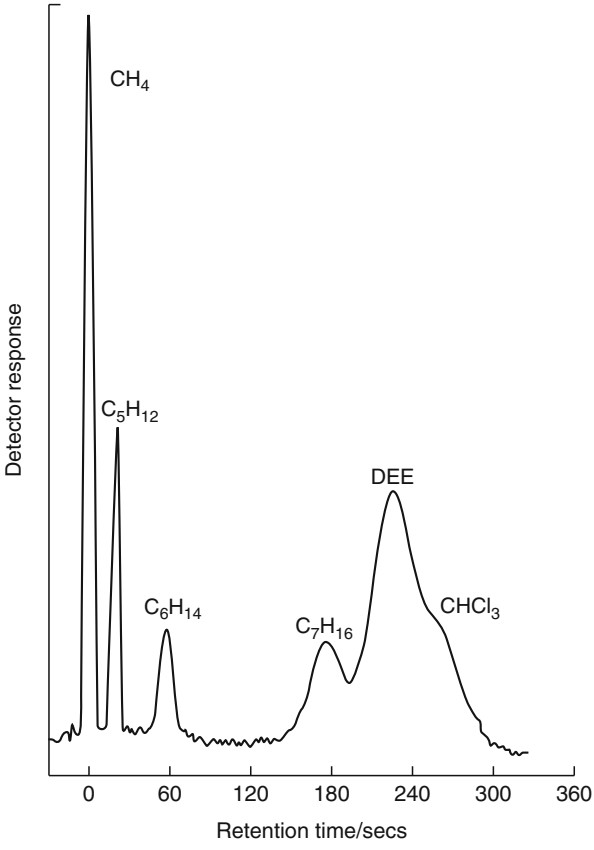

Fig. 9 IGC data recorded for hydrated alumina treated with an organosilane adhesion promoter when five probes are injected simultaneously to illustrate the effect of probe characteristics on retention time (Reproduced from Chehimi et al. 2001 with permission of The Royal Society of Chemistry)

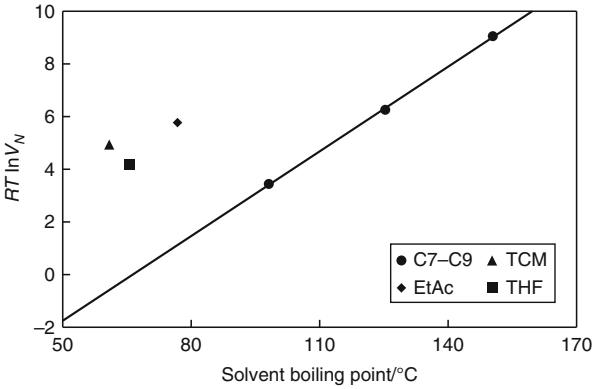

Fig. 10 Adsorption of apolar and acid base probes on an aromatic methacrylate resin. *TCM* chloroform, *EtAC* ethyl acetate, *THF* tetrahydrofuran (Reproduced from Taylor et al. 1995 with permission)

alkane line indicates that the substrate has both acidic and basic sites. This illustrates one of the strengths of IGC; by the informed choice of polar probes it is possible to probe polar sites on the stationary phase and furthermore estimate the extent of acidic and basic contributions.

9.4 Surface Chemical Analysis

As the forces responsible for adhesion between substrate and adhesive or organic coatings operate over very short distances, the requirement for a chemical analysis method that can provide information regarding the nature of interfacial bonding, or indeed the presence of species that will compromise it, along with an exact definition of where failure occurs, needs to have a characteristic sampling depth of similar dimensions. This requirement is met by techniques that fall into the category of those that provide a surface chemical analysis. Although there are a number that can be placed in this category, or other methods that can be modified so as to provide surface-specific information, the term "surface chemical analysis methods" is currently taken to mean three methodologies: X-ray photoelectron spectroscopy (XPS); Auger electron spectroscopy (AES) and its chemical imaging variant scanning Auger microscopy (SAM); and time-of-flight secondary ion mass spectrometry (ToF-SIMS). The methods have all been commercially available for many years and can now be considered as mature analytical techniques that are fairly readily available in universities, corporate research laboratories, and organizations providing contract analysis. XPS and AES are based on the energy analysis of low-energy electrons while SIMS makes use of mass spectrometry of the sputtered surface ions (both positive and negative) to achieve surface mass spectrometry. The analysis depth is of the order of 5 nm for the electron spectroscopies and rather less for SIMS. Their application, particularly of XPS, in adhesion studies has been reviewed by the current author several times in the past (Watts 1988, 2009, 2010) and the current section is intended to provide a very brief overview of these methods and their application in adhesion-related studies. For further details the interested reader is referred to introductory

(Watts and Wolstenholme 2003; Vickerman and Gilmore 2009) or more advanced texts (Briggs and Vickerman 2001; Briggs and Grant 2003) on these topics.

9.4.1 X-ray Photoelectron Spectroscopy

XPS has been widely used in many areas of materials science, chemistry, and physics over the 40 years since it first became commercially available. The application of XPS to adhesive bonding studies and adhesion science in general was well established by the late 1970s and by 1980 there were four research groups with a strong presence in this area, two in the USA and two in Europe, interestingly enough three of these were based in corporate research laboratories with only one in academia (Castle's Group at the University of Surrey). The enthusiasm with which XPS has been adopted by the adhesion community springs, to a large extent, from the important role that surface and interfacial phenomena have to play in the adhesion process. The characteristic length scales over which bonds form, or indeed can be compromised or enhanced by the presence of additional molecules (e.g., contamination or adhesion promoters), are consistent with the analysis depth that is probed by XPS, as well as the other surface analysis techniques.

The heart of the XPS experiment is the irradiation of a solid sample with soft X-rays, usually AlKα with a photon energy of 1486.7 eV. This leads to the emission of photoelectrons that are then injected into an energy analyzer/detector arrangement that will determine their intensity as a function of energy. The primary measurement made by the spectrometer is the kinetic energy (E_k) of the outgoing electrons; this is not a characteristic material property but is a function of the photon energy ($h\nu$) employed in the XPS experiment. The fundamental property is the electron binding energy (E_b), in simple terms the energy with which a particular electron is bound into its electronic orbital. This quantity is related to the experimental observable and photon energy by the following equation:

$$E_b = h\nu - E_k - \omega \tag{5}$$

where ω is a constant term, the spectrometer work function. The output of an XPS system is the X-ray photoelectron spectrum and Fig. 11 indicates the survey spectra obtained from clean aluminum foil and foil that has been handled prior to analysis. The spectra contain peaks that are assigned to Al (2p and 2 s), Si (2p and 2 s–contaminated sample only), C (1 s), and O (1 s); in addition there are Auger transitions associated with the de-excitation of the C1s and O1s core holes. These spectra are readily quantified to provide a surface chemical analysis in atomic percent, the carbon level having doubled on handling and silicon having appeared on the surface at a concentration of 6.3%. The silicon is present as a silicone oil (most likely from a personal care product) and provides an example of the type of adventitious material present on a surface that may compromise the bonding process and the performance of the adhesive joint.

As well as ready quantification XPS can provide chemical state information by inspection of the exact binding energy of the XPS peak. This so-called chemical shift

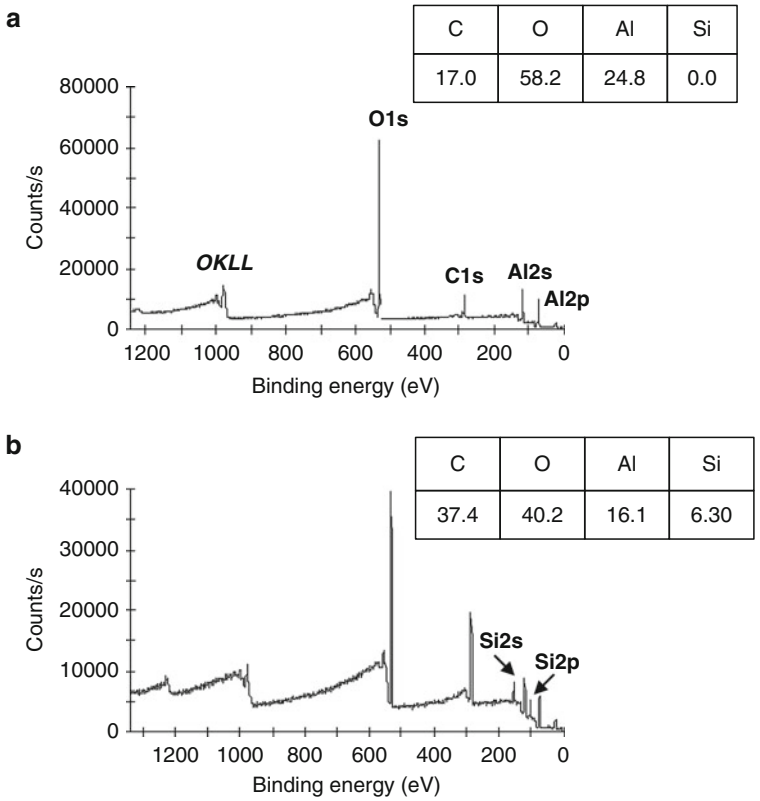

Fig. 11 XPS survey spectra of aluminum foil recorded in the (**a**) as-received condition, and (**b**) following handling contamination. The quantitative surface chemical analyses (in atomic percent) is given in the inset boxes on each spectrum

is the cornerstone of XPS and provides a powerful means of assessing the valence state of metallic and nonmetallic species and the bonding types in organic and polymeric molecules. Figure 12 illustrates this aspect of XPS with a high-resolution Al2p spectrum showing components assigned to metallic aluminum (Al^0) and the oxide (Al^{3+}). The intensity of electrons (I_d) emitted as a function of depth (d) is described by the well-known Beer–Lambert Equation:

$$I_d = I_\infty \exp(-d/\lambda \cos\theta) \tag{6}$$

where I_∞ is the intensity from an infinitely thick sample of the same composition, λ is the electron attenuation length (the effective scattering length of electrons of a particular energy in the solid of interest that will be 1–3 nm), and θ is the electron take-off angle relative to the sample surface normal. The variation of the intensity with depth is shown in Fig. 13, which illustrates quite clearly the exponential decay of the signal as a function of depth. This form represents the intensity for a solid with a thin attenuating overlayer (such as an oxide on a metal) and relates to the signal

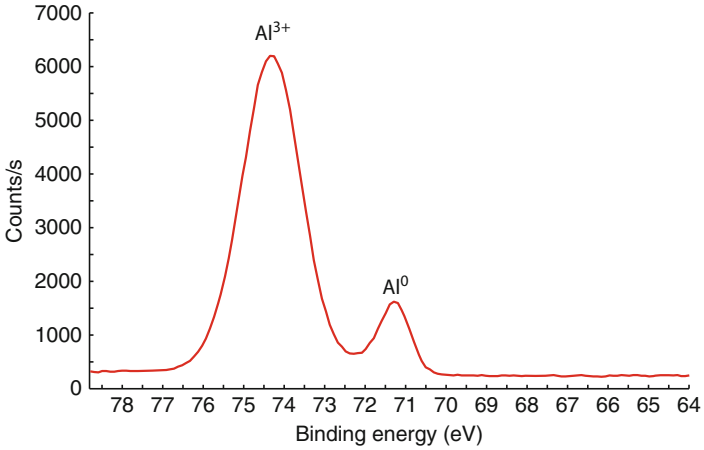

Fig. 12 High-resolution Al2p spectrum showing metallic and oxidic components of the spectrum

from the substrate. The Beer–Lambert Equation can also be written in terms of a thin overlayer (such as the oxide on a metal) where the signal considered is that from the thin overlayer. The equation then becomes:

$$I_{\mathrm{d}} = I_{\infty}[1 - \exp(-d/\lambda \cos\theta)] \tag{7}$$

This provides a useful approach for calculating the thickness of thin layers on substrates such as a thin adhesive residues or the thickness of a contaminant layer. In the case of a thin metal oxide, the two equations can be combined to provide a ready means of estimating the oxide thickness from the intensity of the cationic (I^{ox}) and metallic (I^{me}) components of the spectrum:

$$d = \lambda \cos\theta \ln[(I^{\mathrm{ox}}/I^{\mathrm{me}}) + 1] \tag{8}$$

For the spectrum of Fig. 12, an oxide thickness of 4.2 nm is calculated using this method.

The geometric term, θ, in Eq. 6 indicates the variation of electron yield with the take-off angle and this provides an important way in which the depth of analysis can be varied by recording spectra at different take-off angles. This is known as angle-resolved XPS (ARXPS) and by combining the ARXPS data set with suitable software it is possible to use this method to produce shallow compositional depth profiles in the range 0–5 nm. This is particularly useful for investigating the surface segregation of minor components to free surfaces or, indeed, interfacial failure surfaces.

Thus, XPS provides a quantitative surface analysis method that is applicable to all solid materials, so long as they are stable within the ultra-high vacuum environment of the spectrometer, and the high-resolution spectra provide chemical information for all elements in the periodic table with the exception of hydrogen. Traditionally XPS is considered to be an area-integrating technique as the photoelectron spectrum is

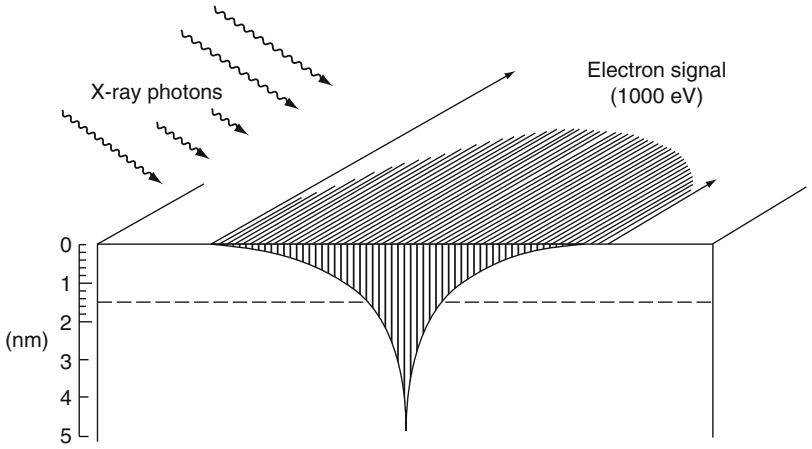

Fig. 13 Variation of electron emission as a function of depth for a typical XPS experiment

acquired over a relatively large area of several square millimeters. Modern instruments, however, are able to record complete spectra at high spatial resolution (the best currently available is 10 μm) or produce elemental or chemical maps similar in appearance to those produced in electron probe microanalysis (EPMA). Such improvements have come about as a result of the development of microfocus X-ray monochromators and analyzers that allow the acquisition, in parallel or serial format, of images at the detector. A current state-of-the-art XPS system will be equipped with a monochromatic AlKα X-ray source and imaging facilities by either parallel (at the detector) or sequential (rastering either specimen stage or X-ray spot) acquisition. The two approaches to imaging XPS both have their advantages; parallel imaging is much faster and allows assessment of the specimen to be made as the XPS images develop, but extraction of chemical state information requires a number of sequential energy-selected maps to be acquired. With serial mapping (analogous to the EPMA approach) a full spectrum can be acquired at each pixel point as the position of analysis moves sequentially across the specimen. The data set can then be integrated and spectra at each pixel point peak fitted or used to contribute to a quantitative analysis or overlayer thickness map. The disadvantage of such a method is that it is very time consuming. Figure 14 illustrates the small spot XPS system in the author's laboratory (which uses serial acquisition for imaging) and provides parallel ARXPS data. The XPS images from a failed adhesive joint obtained with this system are shown in Fig. 15.

9.4.2 Auger Electron Spectroscopy and Scanning Auger Microscopy

AES and SAM are both based on the use of a finely focused electron beam to provide a surface analysis. The division between the two techniques is largely arbitrary nowadays but the configuration of a scanning Auger microscope will have, in appearance,

Fig. 14 Modern XPS system with serial imaging and parallel ARXPS capabilities

much in common with a scanning electron microscope and at its heart will be a high-resolution electron gun, typically giving sub 10 nm resolution, and a high transmission electron energy analyzer. Such systems can usefully form the basis of sophisticated multi-technique instruments and Fig. 16 shows the Auger microscope in the author's laboratory that was specified in this way. As well as featuring high-resolution Auger analysis, this instrument also has facilities for energy dispersive X-ray analysis (EDX), XPS, and backscattered electron detection. The provision of AES and EDX without the need to relocate the sample is extremely useful as it provides analysis in surface and bulk regions (5 nm cf. 1 μm). In contrast to scanning Auger microscopy, AES is taken to mean the provision of electron-induced Auger spectra, often in the form of an ancillary technique on an XPS system (as the analyzer used is the same) or process systems (where deposition quality may need to be monitored) where the need for the ultimate spatial resolution is not paramount. Electron guns for this application will range in spot size from 5 μm down to 100 nm, still much better than the spatial resolution that can be achieved by XPS.

The generation of an Auger electron is a three-electron process involving the removal of a core electron to leave a core hole, the filling of the hole by an electron from outer level and the emission of an electron (often from the same outer level) as an Auger electron. The nomenclature employed for Auger transitions identifies the element and the energy levels involved in the three-electron process, for example, Zn L_3 $M_{4,5}$ $M_{4,5}$. The Auger process achieves the same relaxation effect as the emission of an X-ray photon (indeed they can be considered as competitive processes) but

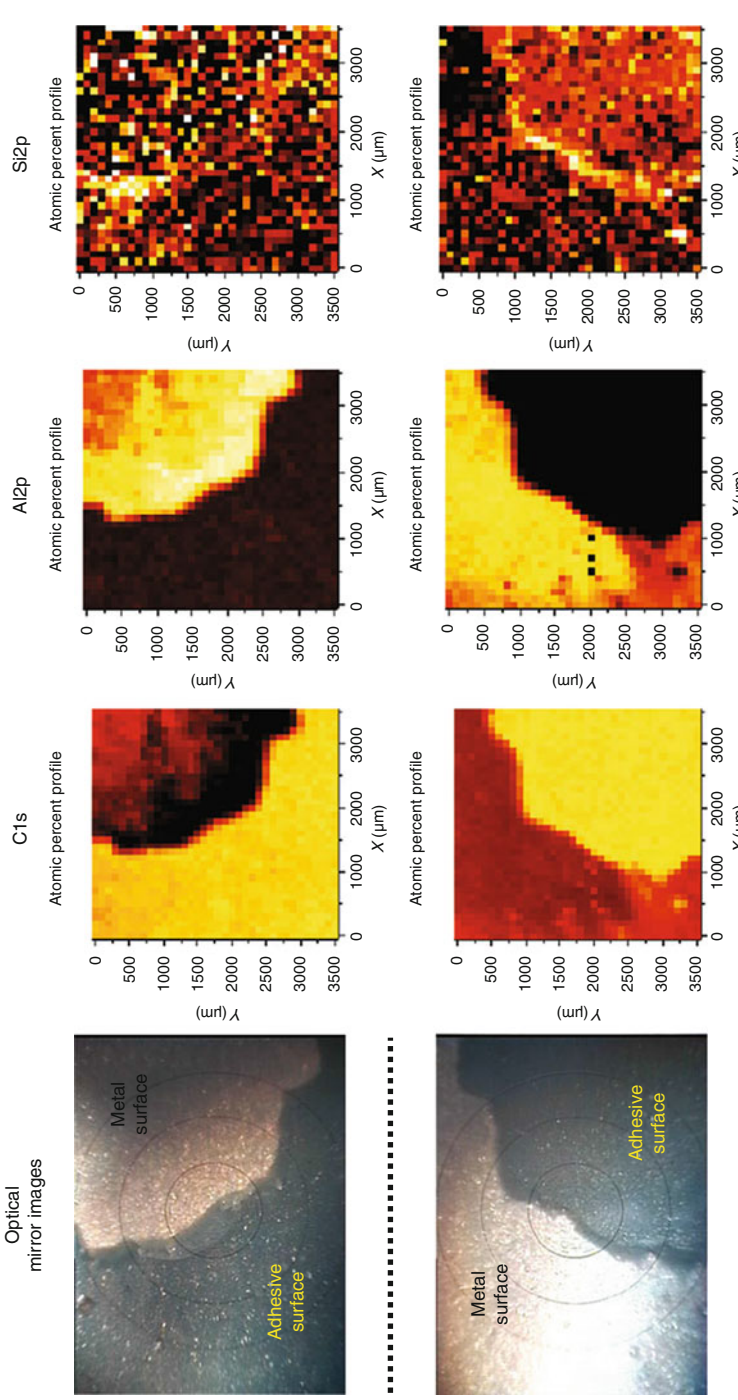

Fig. 15 XPS images recorded from the interfacial failure surfaces of an adhesively bonded aluminum joint, prepared using an organosilane primer, with an instrument of the type shown in Fig. 14. The optical mirror images are complementary views of the fracture surfaces and are mirrored along the dotted line. Visually the failure appears to be interfacial with the fracture path moving from one interface to the other at the boundary between metal and adhesive interfacial failure surfaces

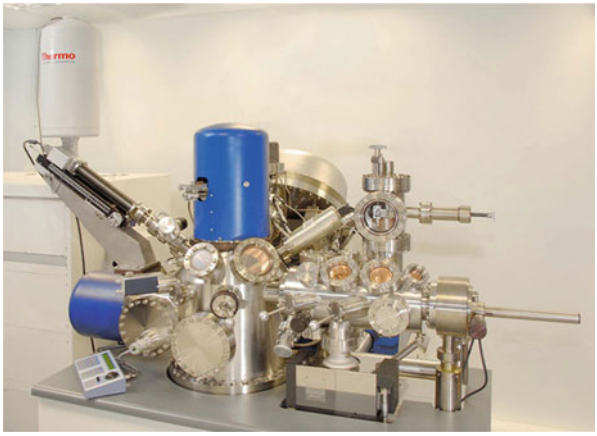

Fig. 16 A multi-technique analytical system (AES, SAM, SEM, XPS, EDX, BSE) based around a high-resolution scanning Auger microscope

fortuitously Auger cross sections are good where X-ray ones are less favorable and vice versa. The nature of the Auger emission process means that very light elements do not show Auger transitions but elements from beryllium onward all yield Auger spectra. As an example of Auger spectra, Fig. 17 shows Auger spectra taken from the points identified in the SEM image of Fig. 1. The two survey spectra show clear differences in the Zn spectra with the data from Point 1 being much better defined than Point 2. The high-resolution Al KLL spectra provide an example of the chemical shift (seen in all elements in XPS), in AES; Point 2 shows both metallic and oxide contributions but Point 1 only shows evidence of aluminum oxide. The Auger chemical effect is generally only observed for transitions in which all three electrons can be considered to be core electrons. If valence band electrons are observed, the band structure is reflected in the shape of the Auger peak that becomes broad and degenerate and yields little chemical information.

It is usual for XPS and AES/SAM systems to be fitted with an inert gas ion gun which can be used for sputtering the surface layers of metallic and inorganic samples. When such sputtering is interspersed with surface analysis it is straightforward to produce a compositional depth profile. Figure 18 indicates a very high quality Auger sputter depth profile obtained from a multilayer structure provided as a standard reference material. In order to get very good interface definition from these 5-nm thick metallic layers, various parameters were optimized including ion beam energy, and specimen geometry, which was rotated during sputtering to avoid the development of ion beam–induced topography. By combining depth profiling with SAM it is possible to obtain a three-dimensional nanoscale representation of the near-surface region of a specimen.

SAM is a technique that can sample extremely small volumes of material (probably the smallest of any technique without the need for extensive sample preparation) and for this reason the choice of sample and the manner in which the analysis is carried out is extremely important. As with any electron microscopy–based analysis method, the need to acquire data from a representative sample of the specimen must be uppermost in the mind of the analyst. As SAM is an electron beam technique it is really only applicable to conductors or semiconductors, a useful guide being that if the specimen

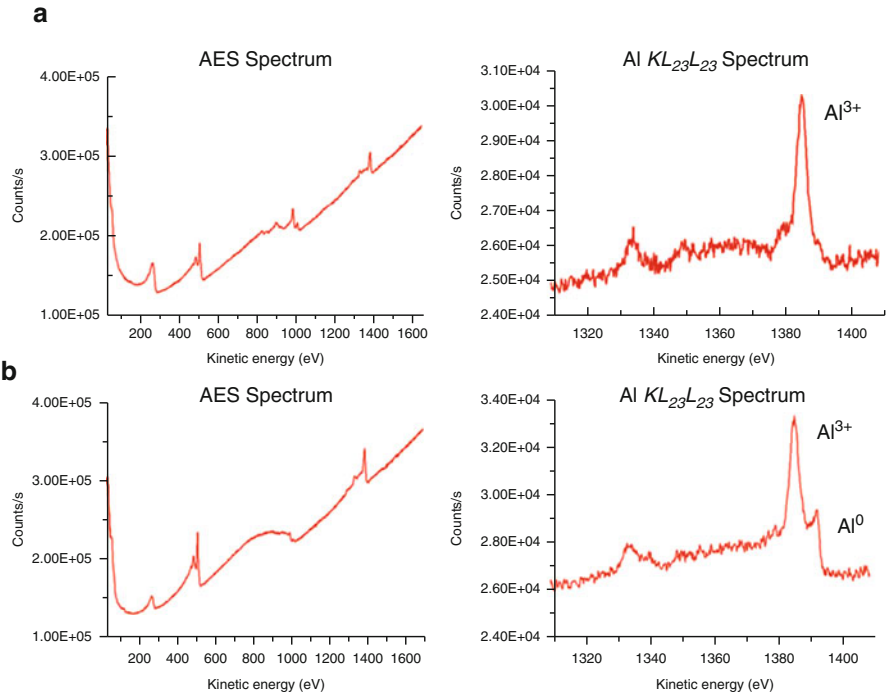

Fig. 17 AES point spectra from the regions identified in the SEM image of Fig. 1. (**a**) Point 1 of Fig. 1, (**b**) Point 2 of Fig. 1

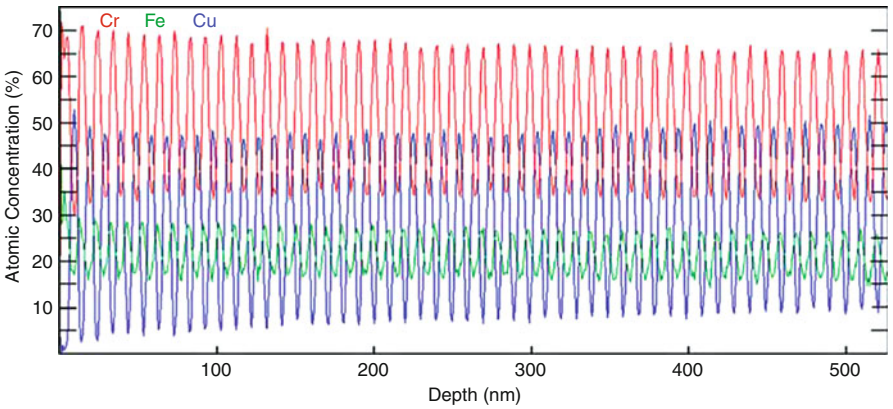

Fig. 18 AES sputter depth profile through an iron/copper/chromium multilayer structure. Each layer is 5 nm thick (Courtesy of Thermo Fisher Scientific)

can be imaged in an SEM without sample charging SAM will be possible. For these reasons the role of AES/SAM in adhesion studies is restricted to the analysis of metallic substrates and pretreatment layers. There are ways in which it is possible to apply the technique to insulators (Baer et al. 2010) but analysis of polymers by AES is not practicable the usual approach being to use XPS or ToF-SIMS.

9.4.3 Time-of-Flight Secondary Ion Mass Spectrometry

In recent years SIMS has become a widening field with many types of ion sources and mass spectrometers being used to provide surface mass spectrometry. In ToF-SIMS the solid sample under investigation is bombarded by a beam of primary ions that sputters atomic ions, cluster ions, and neutrals from the surface. The secondary ions (either cations or anions depending on whether a positive or negative ToF-SIMS spectrum is being acquired) are extracted by high voltage extraction optics and injected into a time-of-flight mass spectrometer. The flight time of the ions is proportional to their mass, once energy distribution has been normalized by the use of an ion mirror, and the time taken to reach the detector is then converted to mass to charge ratio. Modern ToF-SIMS systems can operate at extremely high mass resolution and peak positions can be recorded with an accuracy of ± 0.001 Da, and this together with high transmission and parallel detection of all masses makes this analyzer the one of choice for surface analysis by SIMS. It should be noted that Dalton (Da) is the preferred unit in mass spectrometry indicating unified mass/charge (m/z). The unified mass unit is not the same as atomic mass unit as the former is relative to the ^{12}C isotope while the latter is relative to the ^{16}O isotope. The difference between the two however is small at 318 ppm. As the SIMS process is a destructive one, in that material is removed from the surface as it is irradiated with the primary ions, by collecting the secondary ion signals as a function of sputter time it is possible to construct a compositional depth profile. This forms the basis of a technique known as dynamic SIMS, used for profiling dopant concentration in semiconductors and the like. For surface analysis by SIMS it is important that the spectrum is recorded from the undisturbed surface and the general rule of thumb is that the surface remains in this state if the total ion dose during the acquisition of the spectrum is $<10^{13}$ ions cm^{-2}. When SIMS is carried out under these conditions it is known as static SIMS and the critical ion dose is referred to as the static limit.

A top end ToF-SIMS instrument, of the type shown in Fig. 19, is a very complex analytical system that provides the analyst with many choices relating to the manner in which the spectrum or image is acquired. Does one optimize spectral resolution or spatial resolution? Which ion source should be employed as the primary beam and, if required, which for sputtering to produce a depth profile? One of the key decisions to be made is in the choice of ion source; this can be monoatomic in nature (e.g., Ga^+, Bi^+, Cs^+, Ar^+), but a major advance over the last decade has been the routine availability of cluster (i.e., polyatomic) ion sources. These are particularly useful in the ToF-SIMS analysis of polymers as they increase the yield at high masses and there is also increasing evidence that they increase the yield of nitrogen-containing

Fig. 19 A modern ToF-SIMS instrument featuring multiple ion sources and preparation chamber

fragments (which occur at even masses if there are an odd number of nitrogen atoms in the cluster), which is particularly useful for the analysis of amine-cured epoxy adhesives. The choice of cluster ions available from ToF-SIMS manufacturers is currently based around liquid metal ion sources for high spatial resolution; for example, a bismuth source of this type can provide elemental ion (Bi^+) or Bi_3^+, Bi_5^+, or Bi_7^+ cluster ions. There is a very slight reduction in spatial resolution of bismuth trimers compared with elemental ions, the best available currently being of the order of 100 nm. The other cluster ion source that has gained increasing popularity in the last few years is Buckminster Fullerene, C_{60} and while the resolution is of a few micrometers it is widely used as a primary source in biological studies although the mode of operation preferred for polymeric samples is to use the C_{60} source for sputtering and the Bi source for analysis. This combination indicates one of the strengths of the C_{60} source, which is its ability to sputter profile some polymeric materials without the damaging effects that are normally observed when profiling with inert gas ions such as Ar^+. Such profiling can be carried out by XPS as well but is restricted to certain commercial systems, whereas in ToF-SIMS the depth profiling of polymers is becoming a routine undertaking. Figure 20 illustrates such a depth profiling experiment on a poly(vinylidene fluoride) coating to which an acrylic flow aid had been added. The negative ToF-SIMS spectrum (Fig. 20a) was obtained after a short (<500 ms) sputter with 8 kV C_{60} ions. The depth profile of Fig. 20b shows how the acrylic specific ions peak at a sputter time of 1 s and then decreases as the PVdF ions reach a maximum at the same time. Angle-resolved XPS indicates that the surface segregated layer is about 1.5 nm thick so the seven second depth profiles represent about 10 nm in depth. The high-resolution spectra of Fig. 20c, recorded from the acrylate-rich subsurface and the PVdF bulk material from deeper in the profile, indicate the ease with which two ions of nominal mass

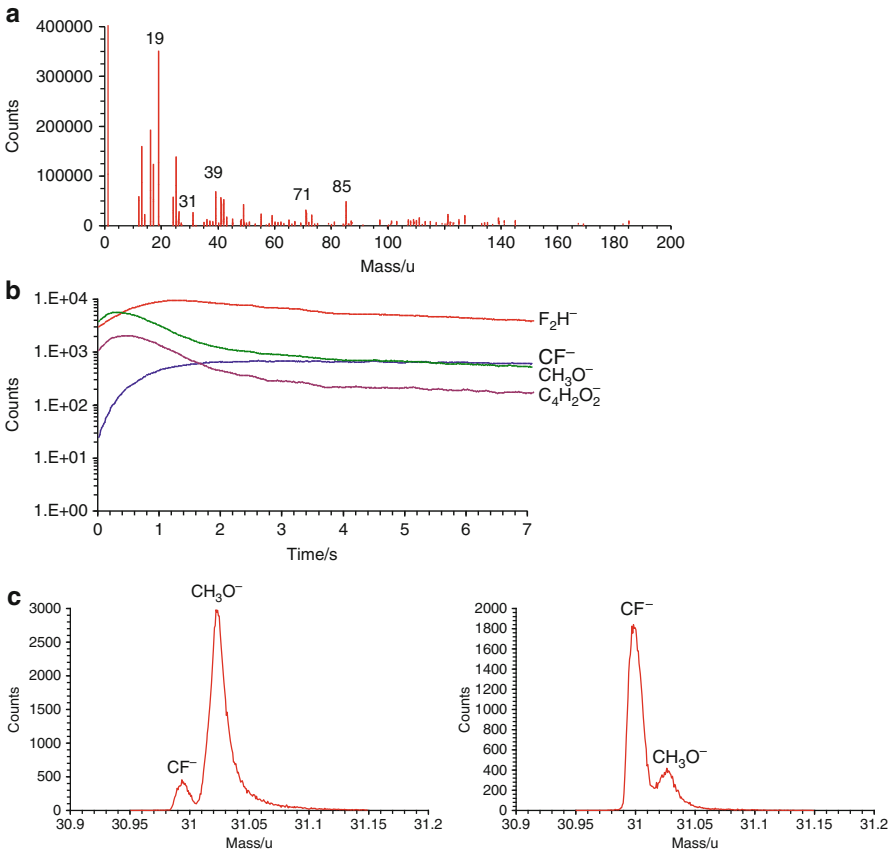

Fig. 20 ToF-SIMS depth profile experiment of a PVdF organic coating. (**a**) Negative ToF-SIMS spectrum from a subsurface region of the materials showing the presence of acrylate ions in the spectrum, (**b**) molecular depth profiling showing PVdF and acrylate specific ions, (**c**) high-resolution negative ToF-SIMS in the nominal 31 u region of the spectrum

31 u can be resolved in the high-resolution mode. The exact masses of the two ions are 30.9984 u (CF^-) and 31.0184 u (CH_3O^-), the separation of 0.02 u quite easily achieved with the experimental conditions used.

ToF-SIMS can also be operated in a mode that provides spatially and mass-resolved chemical images referred to as imaging SIMS. The usual manner of operation is to collect full sets of mass spectra at each pixel point and post-acquisition processing is undertaken to assemble the mass-selected images of interest. A very simple manner in which variations of two mass fragments can be compared is by the use of a scatter ratio diagram, a technique developed many years ago for the processing of scanning Auger microscopy data. In the creation of a scatter ratio diagram, from ToF-SIMS data, two mass-selected images are compared and at each pixel point the intensity of the two ions are plotted on orthogonal axes. This enables the analyst to identify clusters of pixels that have similar compositions. These pixels are then highlighted

on a false color image to enable these regions to be visualized in x:y space. The scatter ratio diagram contains only compositional, but no direct positional, information while the false color image correlates positions of similar compositions. This can be illustrated by data obtained from a galvanized steel sample similar to that illustrated in Fig. 1. ToF-SIMS data was acquired in the usual way from a region 500 × 500 μm in size. The intensity of the $^{27}Al^+$ and $^{64}Zn^+$ ions were compared at each pixel point and the scatter ratio diagram of Fig. 21 produced. From this diagram it can be seen that the data falls into two distinct regimes, those with a low $^{64}Zn^+$ intensity (outlined in dark gray) and those where the $^{64}Zn^+$ intensity is significantly higher (outlined in light grey). If a false color map is now constructed with pixels in the low zinc region coded dark grey and those from the higher zinc region coded light grey, the characteristic topography of the steel sheet is revealed (Fig. 21b), indicating the regions that are low in zinc (dark grey) and those where the surface zinc concentration is higher (light grey).

Of course as with all forms of microscopy there is the trade-off of spatial resolution with intensity, which, in the case of ToF-SIMS, invariably compromises the spectral resolution. Although the ultimate spatial resolution may be of the order of 100 nm, the spectral resolution at this level will only be around unit mass resolution; if one optimizes spatial resolution the mass resolution has to be degraded to several micrometers in order to get adequate counting statistics. Fortuitously for the analyst instrument manufacturers provide a mode of operation that offers middle ground in forms of both spatial and spectral resolution.

The manner in which a ToF-SIMS data set is collected, with complete spectra at each pixel point, means that a single image, from perhaps a 100 × 100 μm^2 or 500 × 500 μm^2 field of view comprising of a 128 × 128 pixel array, will contain

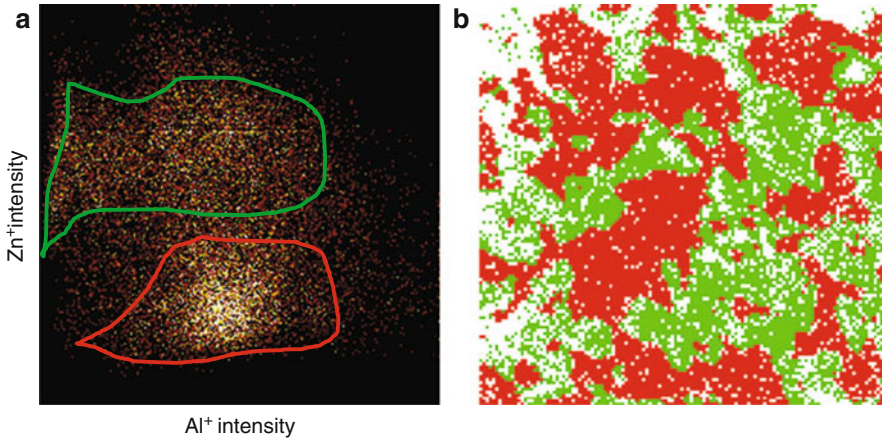

Fig. 21 ToF-SIMS analysis of a galvanized steel sample. (**a**) is the scatter ratio diagram constructed from the intensities of the $^{27}Al^+$ and $^{64}Zn^+$ ions and regions of higher (*light grey*) and lower (*dark grey*) zinc concentration are readily identified, (**b**) grey scale ToF-SIMS image constructed using the dark and light grey regions of Fig. 21a, which now indicates the areas on the sample surface enhanced and deficient in zinc

more than 16,000 individual spectra; added to this is the possibility of depth profiling with 100 analysis points into the sample and the number becomes well over one million in the data set! With so many spectra the examination and interpretation of each individual spectrum becomes impossible; the univariate analysis approach will not work so one must resort to multivariate analysis (MVA) techniques. These are now widely applied in ToF-SIMS as well as many other forms of materials analysis and form part of an area of endeavor known as chemometrics. Commercial ToF-SIMS data systems now have MVA software included, but it is still often necessary for the analyst to buy in specific software suites and adapt for ToF-SIMS use. Popular MVA methods used to process ToF-SIMS data include principal component analysis, multivariate curve resolution, and partial least squares regression. Recent literature in the area has been augmented by an extremely comprehensive review article by Lee and Gilmore (2009) and also a special two-volume issue of the journal *Surface and Interface Analysis* (2009a, b) dealing MVA in surface analysis.

In adhesion research one of the options that has become achievable at last with the latest generation of ToF-SIMS instruments is the ability to track reaction chemistry on surfaces; in this manner it is possible to study how components present in an adhesive formulation may interact with the solid surface, and in this manner it has become possible to start to unravel the interface chemistry of adhesion from very complex multicomponent systems. Other important applications in adhesion include the identification of minor components of an adhesive at fracture surfaces and the ability to visualize such residues at a resolution of significantly less than 1 μm.

9.5 Conclusions

There are a wide variety of procedures and analytical methods that can be used to assess the surface characteristics of a solid surface relevant to adhesive bonding. These range from the relatively simple and inexpensive such as the water break test through to the extremely complex and expensive such as ToF-SIMS. Some will be required for quality assurance purposes and some belong in a research environment; the surface characteristics that require assessment may be surface topography (AFM or SEM might be used), surface energetics (contact angle measurements or IGC), or surface chemical analysis (XPS, AES/SAM, or ToF-SIMS). It is unlikely that any one laboratory will have access to all such techniques and thus those readily available will be pressed into service. Some laboratories will carry out commercial consultancy activities for all-comers and this is often a cost-effective way to obtain electron microscopy and surface analysis services. This is often a way to gain familiarity with advanced techniques and added value is often obtained from experienced analysts who will be responsible for instrument operation.

In order to obtain a clear, concise, and accurate picture of the surface under investigation, there will almost certainly be the need to resort to more than one of the methods described in this chapter. The choice will be influenced by the nature of the material, the type of investigation, and other variables. In adhesive bonding research one thread that runs through virtually all work, be it quality assurance, development,

or research, is to relate surface characteristics to a performance measure of the bonded structure. This may be joint strength or toughness but more usually, and particularly for structural adhesive bonding, attempts will be made to correlate the surface and interface characteristics with joint durability.

References

Abel M-L, Watts JF (2005a) Inverse gas chromatography. In: Packham DE (ed) Handbook of adhesion. Wiley, Chichester, pp 252–254

Abel M-L, Watts JF (2005b) Inverse gas chromatography and acid-base interactions. In: Packham DE (ed) Handbook of adhesion. Wiley, Chichester, pp 255–257

ASTM (2002) F 22–02 Standard test method for hydrophobic surface films by the water break test. ASTM, West Conshohocken

Baer DR, Lea AS, Cazaux J, Geller JD, Hammond JS, Kover L, Powell CJ, Seah MP, Suziki M, Wolstenholme J, Watts JF (2010) J Elec Spec 176:80–94

Binnig G, Rohrer H, Gerber C, Weidel E (1982) Phys Rev Lett 49:57

Briggs D, Grant JT (2003) Surface analysis by Auger and x-ray photoelectron spectroscopy. IM Publications and Surface Spectra, Chichester

Briggs D, Vickerman JC (2001) ToF-SIMS: surface analysis by mass spectrometry. IM Publications and Surface Spectra, Chichester

Brighton Technologies Group Inc (2010) http://www.btgnow.com/SEP.html

BSI (2010) British Standard 1134:2010, Assessment of surface texture. Guidance and general information

Castle JE (2008) J Adhes 84:368

Castle JE, Zhdan PA (1997) J Phys D Appl Phys 30:722

Chehimi MM, Abel M-L, Watts JF, Digby RP (2001) J Mater Chem 11:533

Choi JW (2003) The plasma treatment of poly(dimethylsiloxane) for enhanced surface properties. PhD thesis, University of Surrey

Dillingham RG, Oakley BG, Renieri M, Salah L (2010) From bond gap thickness effects to geometric transferability of fracture parameters in structural adhesives. In: Proceedings 33rd annual meeting of the adhesion society inc, Daytona Beach, 21–24 Feb 2010, pp 217–219

Goodhew PJ, Humphreys J, Beanland R (2001) Electron microscopy and analysis, 3rd edn. Taylor & Francis, London

Lee JLS, Gilmore IS (2009) The application of multivariate data analysis techniques in surface analysis. In: Vickerman JC, Gilmore IS (eds) Surface analysis: the principal techniques. Wiley, Chichester, pp 563–612

Packham DE (2005) Surface energy components. In: Packham DE (ed) Handbook of adhesion. Wiley, Chichester, pp 517–520

Surface and Interface Analysis (2009a) Special issues on multivariate analysis 41(Pt 1):75–142; (2009b) 41(Pt II): 633–703

Surface Measurement Systems (2010). http://www.thesorptionsolution.com/Products_IGC.php

Taylor AM, Abel M-L, Watts JF, Chehimi MM (1995) Int J Adhes Adhes 15:3

Venables JA (1984) J Mater Sci 19:2431

Vickerman JC, Gilmore IS (2009) Surface analysis: the principal techniques. Wiley, Chichester

Watts JF (1988) Surf Interface Anal 12:497

Watts JF (2009) Adhesion science and technology. In: Riviere JC, Myhra S (eds) Handbook of surface and interface analysis: methods for problem solving. CRC Press, Boca Raton, pp 5651–5656

Watts JF (2010) Role of corrosion in the failure of adhesive joints. In: Richardson JA et al (eds) Shreir's corrosion, vol 3. Elsevier, Amsterdam, pp 2463–2481

Watts JF, Wolstenholme J (2003) An introduction to surface analysis by electron spectroscopy. Wiley, Chichester